

HELICAL PILE-TO-PILE CAP CONNECTIONS SUBJECTED TO UPLIFT FORCES: IMPROVING FUTURE PRACTICE

Sundar Chiluwal, The University of Toledo, OH, 567-970-1840, Sundar.Chiluwal@rockets.utoledo.edu
Serhan Guner, The University of Toledo, OH, USA, 419-530-8133, Serhan.Guner@utoledo.edu

Abstract. Although significant research has been conducted on helical piles, there is a lack of research and official design provisions on the helical pile-to-pile cap connections. These connections may govern the global response of pile cap systems—especially in tall and light structures where uplift forces dominate the response. To improve future industry practice, the objective of this study is to understand the influence of pile-to-pile cap connections on the global behavior of concrete pile caps and develop recommendations for their efficient design. For this purpose, 108 high-fidelity nonlinear finite element simulations are conducted to quantify the influences of bracket type, embedment depths, longitudinal reinforcement percentages, shear span-to-depth ratios, and loading conditions on the load, deformation, cracking, and failure behavior of concrete pile caps. The results indicate that the design configurations involving single bracket type may result in premature concrete cracking around the anchorage zones with a 25% reduction in the uplift load capacity. The investigations also confirm that high reinforcement percentages and low shear span-to-depth ratios result in higher load resistance in all bracket types, and that the load capacities of the double and studded bracket types are similar. For applications requiring the use of lower embedment depths, it is recommended that either double or studded bracket types be used. The research findings have applicability to both helical and micro piles given that both include similar connection types.

Keywords: Helical pile, helical pile-to-pile cap connections, single bracket type, double bracket type, studded bracket type, longitudinal reinforcement (ρ_s), embedment depth (h_e), shear span-to-depth (a/d) ratio

INTRODUCTION

Tall and light structures may experience significant uplift forces at their foundations due to large overturning moments from wind or other lateral loads. Helical piles (e.g., Fig. 1a) can provide a cost-effective, practical, and resilient solution for resisting significant uplift forces. In order to realize the full potential of helical piles, it is imperative that the helical pile-to-pile cap connections (see Figs. 1b, c and d for examples) are properly designed to resist the applied forces. However, there is a lack of research and associated knowledge on the influence of pile-to-pile cap connection detailing on the global response of pile caps.

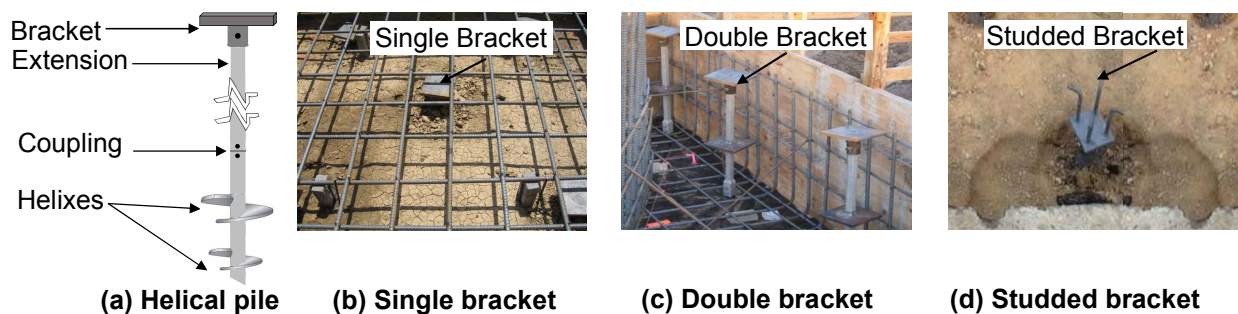


Fig. 1. Helical pile-to-pile cap connections with different bracket types

The geotechnical literature primarily focuses on the axial load behaviour of isolated piles, and consistently demonstrates the suitability of helical piles for load cases including the tensile uplift loads (e.g., Elkasabgy and El Naggar 2013; Cerato and Victor 2009; Livneh and El Naggar 2008; El Naggar et al. 2007; Youssef

et al. 2006) and the compression loads (e.g., Elsherbiny and El Naggar 2013). The structural literature, on the other end, exclusively focuses on the behaviour of traditional pile caps supported by socketed piles, subjected to compression loads (e.g., Cao 2009; Suzuki and Otsuki 2002; Suzuki et al. 2000; Otsuki and Suzuki 1996; Adebar et al. 1990). There is a lack of understanding and official design guidelines for creating safe and efficient helical pile-to-pile cap connections. An experimental study conducted by Diab (2015) demonstrated that the connection behavior might govern the entire system response. In another study, Labuda et al. (2013) investigated the failure of an Olympic-size swimming pool supported by helical piles and found that the pool collapsed due to the connection failure under uplift water pressure. These examples highlight the importance of understanding and explicitly accounting for the connection response when designing foundation systems.

Objectives

In the theme of improving the future practice of helical pile connection design, the objective of this study is to understand the effectiveness of the commonly-used bracket types (e.g., Fig. 1) and predict their load, deformation, cracking, and failure behavior using state-of-the-art high-fidelity nonlinear analysis methods. For this purpose, 108 high-fidelity nonlinear finite element (NLFE) simulations are conducted to understand and quantify the influences of bracket type, embedment depths (h_e), longitudinal reinforcement percentages (ρ_x), shear span-to-depth (a/d) ratios, and the loading conditions (uplift and compression). A significant emphasis is placed on understanding the behavior of connections under *tensile uplift* (i.e., *pullout*) loads, as opposed to compression loads, and identifying undesirable failure modes and design configurations.

PILE CAP MODEL PARAMETERS

A foundation strip representative of commonly-used pile cap configurations (e.g., strip footings, grade beams, or a segment of pile caps) was designed, following the CRSI (2015) and Guner and Carriere (2016) recommendations. The strip is supported by two helical piles to create a one-way stress flow and better isolate the pile cap response (see Fig. 2). Helical piles are terminated with one of the three bracket types; namely, single bracket (see Fig. 2a), double bracket (see Fig. 2b), and studded bracket (see Fig. 2c). The square helical pile shaft supports the pile cap strip with dimensions of 2100 mm x 800 mm x 600 mm, where the compressive strength of the concrete is 20.7 MPa. The single bracket type has a Grade 50 plate with a size of 254 mm x 254 mm and 19-mm thick. The double and studded bracket types have plates with the same dimensions and properties to facilitate comparisons with the single bracket type. The studs are No.6 steel rebars of Grade 60. The pile cap strip supports the column load anchored by the bolts of Grade 105 steel, spaced 400 mm, with the length and the diameter of 460 mm and 38 mm, respectively.

Influencing parameters investigated include: three h_e for single bracket type [i.e., 460 mm (top), 300 mm (middle), 140 mm (bottom)]; one h_e for double bracket type [i.e., 460 mm (top)]; two h_e for studded bracket type [i.e., 300 mm (middle), 140 mm (bottom)]; three ρ_x for all bracket types [i.e., minimum 0.2% (5-#5 rebars) from ACI (2014), 0.4% (7-#6 rebars), and 0.8% (10-#7 rebars)]; and three a/d ratios for all bracket types [i.e., 1.68, 1.42, and 1.11] (see Fig. 2). When also considering two loading conditions, 108 pile cap design configurations were created [i.e., $3 \times 3 \times 2 \times (3+2+1) = 108$].

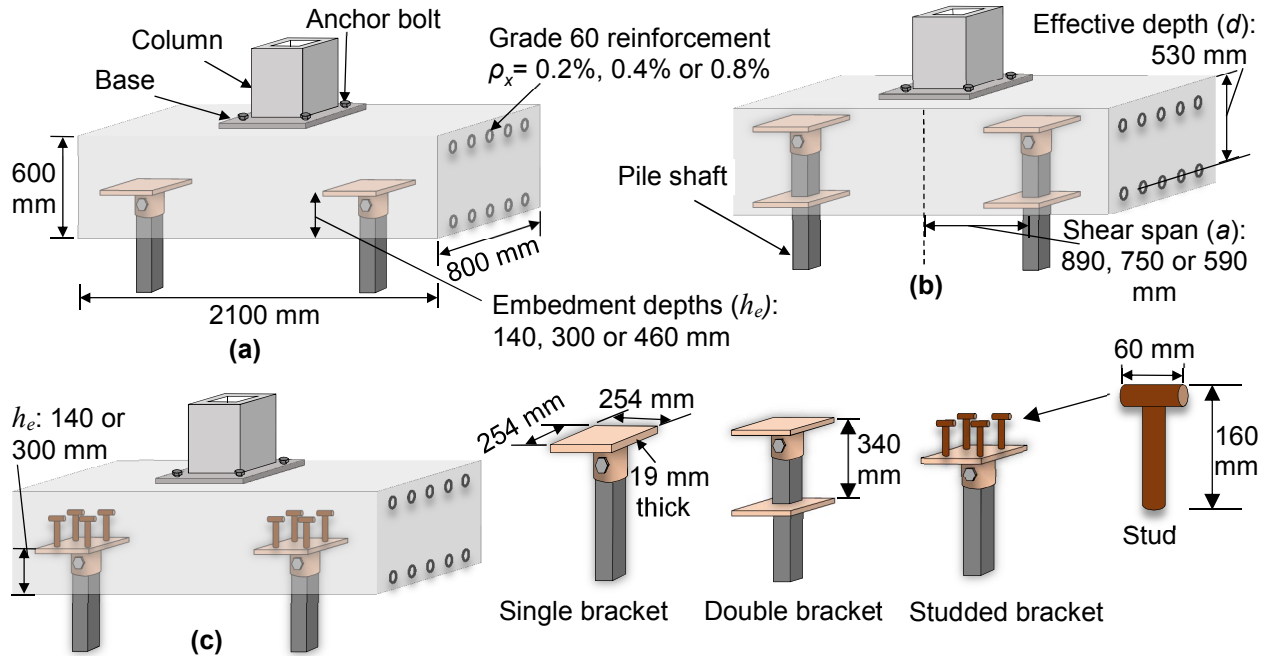


Fig. 2. Helical pile-to-pile cap connections for (a) single bracket type; (b) double bracket type; and (c) studded bracket type

NONLINEAR FINITE ELEMENT MODELING

A two-dimensional, continuum-type, plane-stress element is used for the finite element modeling through a computer program VecTor2 (VTAG 2019). The formulation is based on the Disturbed Stress Field Model (Vecchio 2000), which is an extension of the Modified Compression Field Theory (MCFT) (Vecchio and Collins 1986). The MCFT employs a smeared, rotating crack approach within a total-load, secant-stiffness solution algorithm and allows the consideration of the coupled flexure, axial, and shear effects.

One sample numerical model created is shown in Fig. 3a, where the concrete was modeled using a four-noded rectangular element with 8 degrees of freedom (see Fig. 3b), and the longitudinal reinforcement was modeled using a two-noded truss bar (see Fig. 3c) with 4 degrees of freedom.

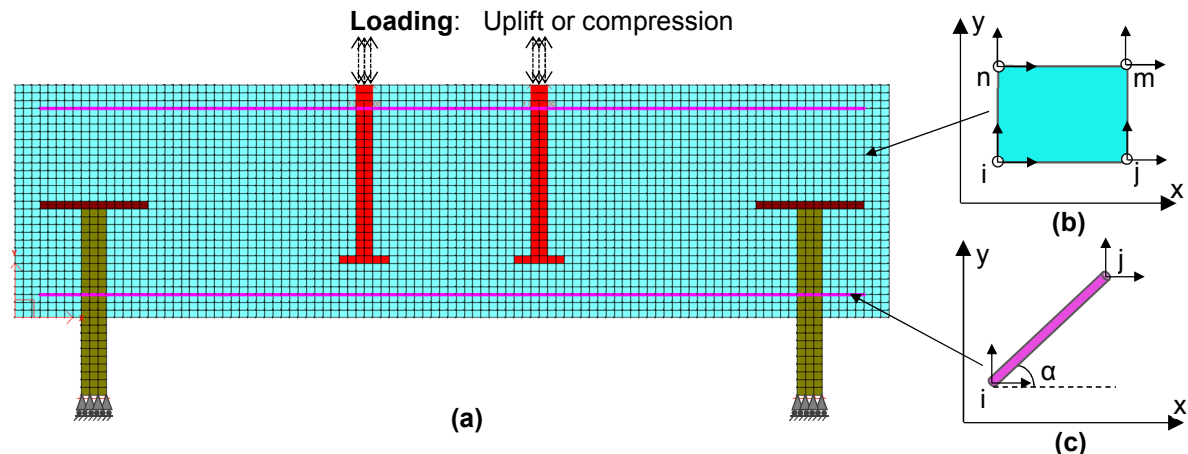


Fig. 3. (a) NLFE model developed in the study for the single bracket type; (b) Plane-stress rectangular element used; and (c) Truss bar element used

Tables 2 and 3 show the component properties in terms of their strengths and dimensions. VecTor2 incorporates several second-order material behaviors (Wong et al. 2013; Akkaya et al. 2019) as listed in Table 4, including the material responses shown in Figs. 4a and 4b as examples. A very fine mesh with a size of 20 mm x 20 mm was used where each helical pile was restrained with four hinges, to better isolate the pile cap response. A displacement-controlled analysis was employed, which is advantageous when simulating the post-peak response, ductility, crack patterns, and failure modes. A monotonic loading was applied uniformly with a displacement increment of 0.2. Sample models of double and studded bracket types are shown in Fig. 5.

Table 2. Continuum region properties

Region	Description	Color	f'_c (MPa)	f_y (MPa)	Thickness (mm)
1	Concrete		20.7	-	800
2	Helical Pile			552	44
3	Bracket Plate		-	345	260
5	Anchor Bolts		-	724	57

Table 3. Truss bar properties

Truss	Description	Color	f_y (MPa)	ρ_x
1	Longitudinal bars		414	0.2%, 0.4% or 0.8%

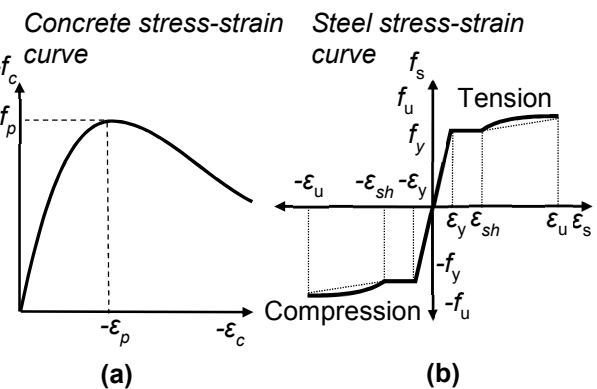
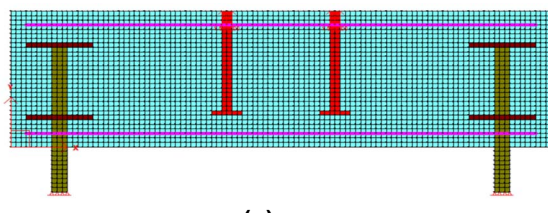


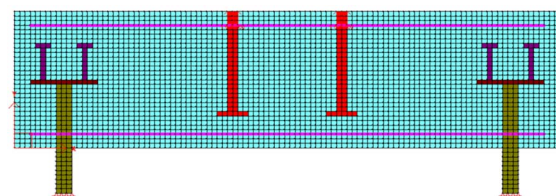
Fig. 4. Two of the material behaviors models used

Table 4. Concrete and reinforcement material models

Material Behaviour	Default Model	Material Behaviour	Default Model
Compressive Base Curve	Hognestad	Concrete Dilation	Variable-Isotropic
Compression Post-Peak	Modified Park-Kent	Cracking Criterion	Mohr-Coulomb (Stress)
Compression Softening	Vecchio 1992	Crack Width Check	Agg/5 Max crack width
Tension Stiffening	Modified Bentz 2003	Crack Slip	Walraven
Tension Softening	Linear	Hysteretic Response	Bauchinger Effect (Seckin)
Confined Strength	Kupler/Richart	Dowel Action	Tassios (Crack Slip)
Buckling	Akkaya et al. 2019		



(a)



(b)

Fig. 5. Numerical models representing top h_e with a/d ratio of 1.68 (a) Double bracket type; and (b) Studded bracket type

UPLIFT BEHAVIOR

The overall uplift responses of all three bracket types are shown in Fig. 6. The maximum load capacities obtained are the same as all bracket types except the bottom h_e of the single bracket type, which provided a 15% less load capacity (see Fig. 6a) due to connection failures. A similar trend is observed for the failure displacements, with the bottom embedment depth sustaining failures under smaller deformation levels.

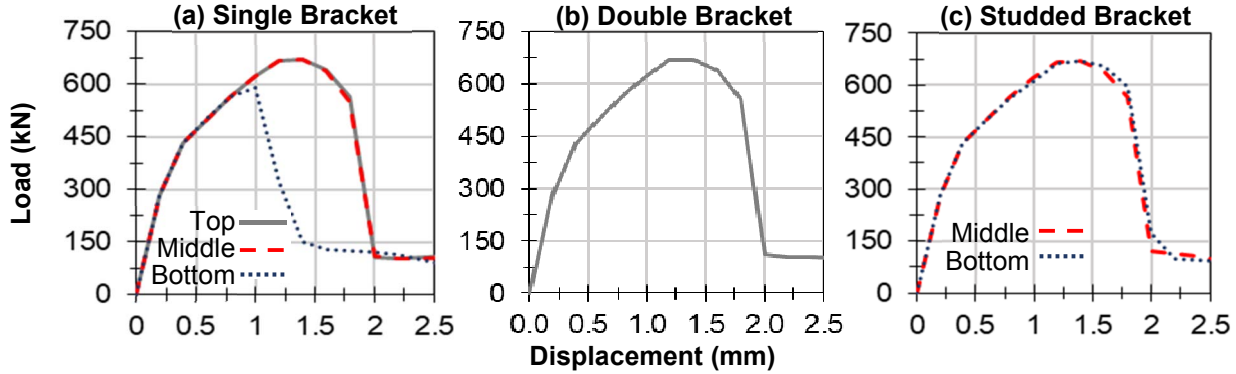


Fig. 6. Simulated responses for a/d ratio of 1.68 and ρ_x of 0.4% subjected to uplift

Figure 7 presents all 54 simulation results in terms of load capacities, h_e , a/d ratios, and ρ_x percentages subjected to uplift. The slopes of three blue lines (i.e., bottom h_e) in Fig. 7a are significantly lower than those of red (i.e., middle h_e) and gray lines (i.e., top h_e), which shows that the capacity increase is much smaller in bottom h_e when a/d ratio is reduced (i.e., pile cap is made deeper) or ρ_x percentage is increased as compared to other h_e . When the h_e is changed from bottom to middle, the capacity increases by an average of 32%. The further increase in h_e from middle to top does not affect the capacity, as shown by the overlapping of red and gray lines in Fig. 7a. The double bracket behaves similarly to the middle or top h_e of the single bracket, as their load capacities are similar (see Fig. 7b). For studded bracket type, the gray lines overlap the blue lines, which shows that the change in h_e does not influence the load capacity (Fig. 7c). Also, the capacity of the bottom or middle h_e for studded bracket type is found to be similar to those of the middle or top h_e of the single bracket type (compare Figs. 7a and 7c). If the bottom h_e must be used, the change of the bracket type from single to studded can improve the global capacity by an average of 29%.

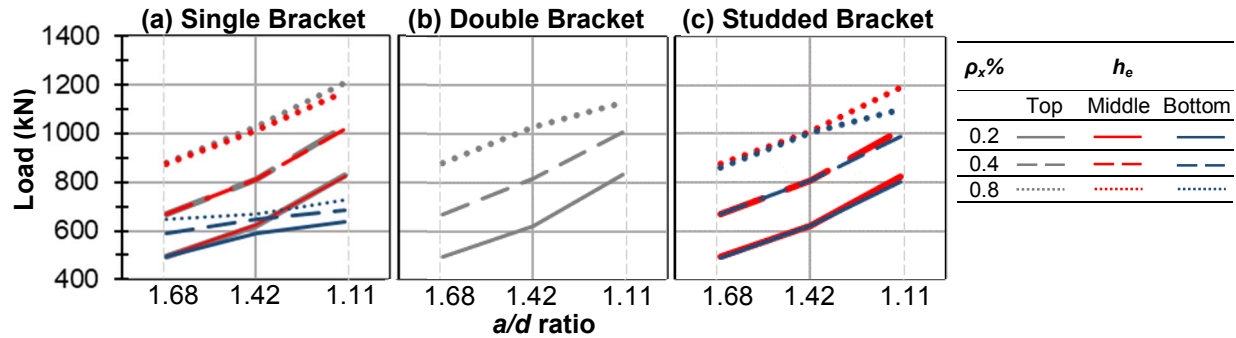


Fig. 7. Interaction among different parameters subjected to uplift.

The uplift capacity of all bracket types increases with higher ρ_x and lower a/d ratios (as shown by the increasing slopes in Fig. 7). For the single bracket type, the capacity increases by an average of 24% and 19% when the ρ_x is increased from 0.2% to 0.4% and 0.4% to 0.8%, respectively, and the capacity increases by an average of 17% and 19% when the a/d ratio is decreased from 1.68 to 1.42 and 1.42 to 1.11,

respectively. Other bracket types exhibit similar increase of capacity for h_e and a/d ratio change within a range of $\pm 5\%$.

COMPRESSION BEHAVIOR

The overall compression responses of all three bracket types are shown in Fig. 8. The maximum load and deformation capacities obtained are the same as all bracket types.

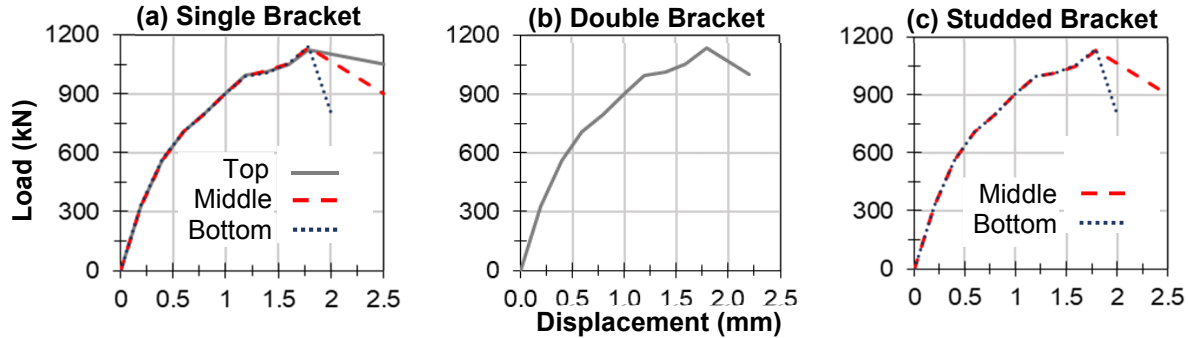


Fig. 8. Load-displacement responses for a/d ratio of 1.68 in ρ_x of 0.4% subjected to compression

Figure 9 presents all 54 simulation results in terms of load capacities, h_e , a/d ratios, and ρ_x percentages subjected to compression. The overlapping nature of lines with different colors demonstrates that the compressive load resistance is independent of the changes in h_e . This can be attributed to the absence of connection failures subjected to compression loading. The load capacity of all bracket types increases with the increase in ρ_x and decrease in a/d ratios. This increase is more pronounced for the lowest ρ_x , as apparent from the bilinear nature of the solid lines in Figs. 9a, 9b, and 9c. When the a/d ratio is changed from 1.42 to 1.11, the capacity increases for ρ_x of 0.2, 0.4, and 0.8 percentages are 43%, 29%, and 19%, respectively. For the single bracket type, the compressive capacity increases by an average of 24% when ρ_x is increased from 0.2% to 0.4%, or 0.4% to 0.8%, while the capacity increases by an average of 21% and 29% when the a/d is decreased from 1.68 to 1.42, and 1.42 to 1.11, respectively. The double and studded bracket types show similar increases in the load capacities within a range of $\pm 5\%$ for similar changes in h_e and a/d .

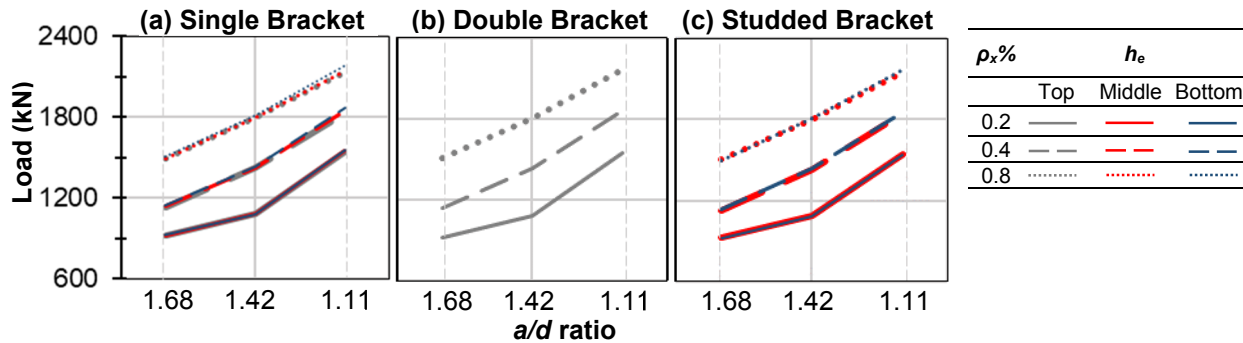


Fig. 9. Interaction among different parameters subjected to compression

DEFORMATION AND CRACK PATTERNS

Dominant concrete cracks are predicted around the connection zone for the bottom h_e of the single bracket type subjected to uplift loads (see Fig. 10a). Connection concrete cracks are concentrated over a small area and extended along the bottom longitudinal reinforcement. This type of failure is found to be the least preferable failure mode in this study because it results in a premature failure with no to very little redistribution of stresses. For the middle or top h_e , concrete cracking only along the top longitudinal

reinforcement are predicted (see Fig. 10b). This type of behavior provided better load redistribution and higher displacement ductility. Other parameters (i.e., ρ_x and a/d ratios) are found to not change the failure modes of the single bracket type. This confirms that h_e is the most influencing parameter for the single bracket type. For the double bracket type, the crack patterns are predicted to be the splitting of concrete along the top longitudinal reinforcement in most of the cases (see Fig. 10c). In the configuration involving higher ρ_x of 0.8% (see Fig. 10d), additional minor anchorage cracks are predicted, yet these cracks are found to not influence the global response of the pile caps in any significant way. For the studded bracket type, a similar cracking behavior is obtained (see Figs. 10e and 10f).

For all the bracket types subjected to compression loads, most of the failure modes involved splitting of the concrete along the bottom reinforcement (see Fig. 10g) where the cracks initiate from the tip of the anchor bolts and propagate to the helical pile anchorages. For the lowest a/d ratio of 1.1 with ρ_x of 0.4% or 0.8%, shear failures are predicted (see Fig. 10h). No signs of anchorage cracks are predicted in any of the brackets.

For all simulations, widespread concrete cracking is found to provide a more favorable global pile cap response than those from concentrated concrete cracking (e.g., Fig. 10a).

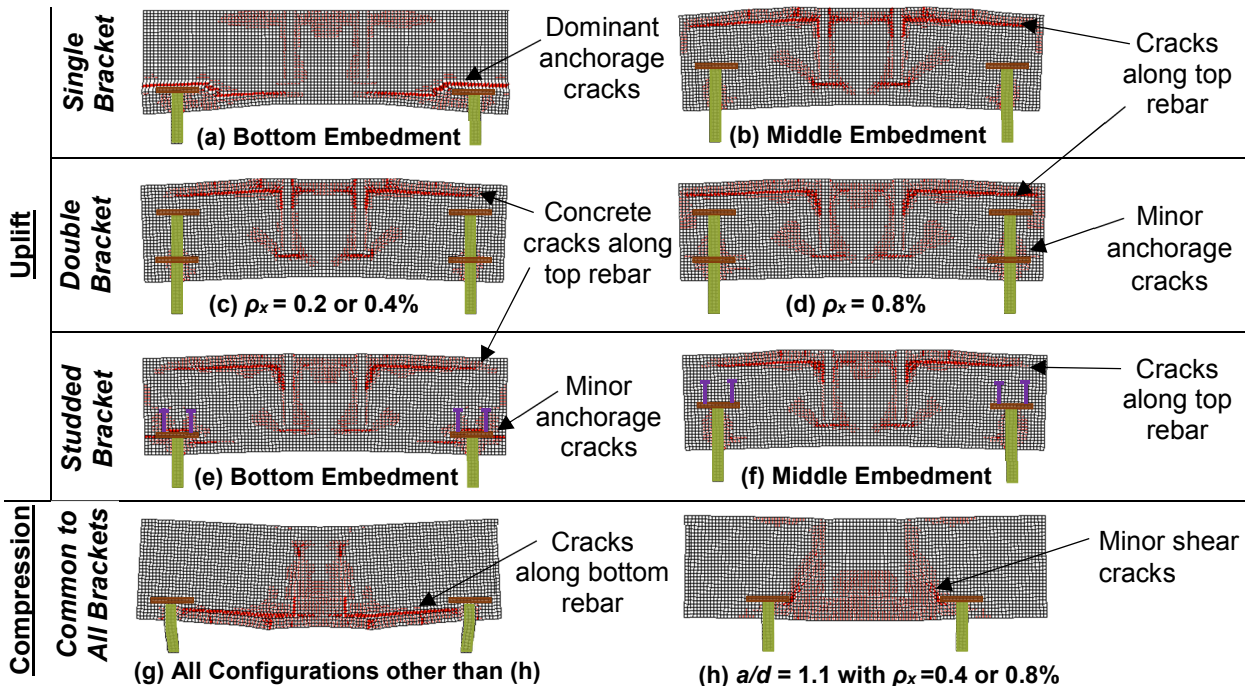


Fig. 10. Failure modes and crack patterns

SUMMARY AND CONCLUSIONS

This study performed 108 high-fidelity NLFE simulations to quantify the influences of key design parameters on the load, deformation, cracking, and failure response of concrete pile caps supported by helical piles. The analyses investigated: the influences of three bracket types (i.e., single, double, and studded); three embedment depths ($h_e = 140, 300$, and 460 mm); three longitudinal reinforcement percentages ($\rho_x = 0.2, 0.4$ and 0.8); and three shear span-to-depth ratios ($a/d = 1.68, 1.42$ and 1.11).

The results of the numerical investigations demonstrate that the helical pile-to-pile cap connections may govern the entire system capacity for the load conditions involving uplift forces. As such, it is recommended to perform an explicit check of the connection capacity in addition to the structural and geotechnical checks for the global pile cap and helical pile capacities. The findings of this study are also applicable to micro piles which incorporate similar connection details. Detailed conclusions and recommendations are provided below for uplift and compression load cases.

Uplift Behavior

- Connection (anchorage) failure is predicted only for the bottom h_e of single bracket type, which decrease the global tensile load resistance of the pile cap by an average of 25%. It is recommended that the bottom h_e should be avoided for the most efficient design when the single bracket type is used.
- The analysis indicates that h_e is the most influential parameter, which also dictates the effectiveness of ρ_x and a/d ratio on the uplift load resistance for the single bracket type.
- The uplift load capacity increases by an average of 29% when h_e is changed from bottom to middle for the single bracket type.
- The uplift load capacity remains similar when h_e is changed from middle to top for the single bracket type. Therefore, it is still recommended to use the middle h_e .
- The uplift load capacity increases by an average of 22% when ρ_x is increased from 0.2% to 0.4% or 0.4% to 0.8% for the single bracket type.
- The uplift load capacity increases by an average of 18% when the a/d ratio is decreased from 1.68 to 1.42 or from 1.42 to 1.11 for the single bracket type.
- The double bracket type has only one h_e , which provides satisfactory response with no anchorage failure. The load capacity increases similar to the single bracket type for ρ_x or a/d ratio changes.
- The studded bracket type has two h_e positions, and the change in h_e does not influence their capacities. Any one of these embedment depths could be used for efficient design. The load capacity increases similar to the single bracket type for ρ_x or a/d ratio changes.
- For the configurations involving bottom h_e , the change of bracket type from single to studded improves the pile cap capacity by 29%. Therefore, if the bottom h_e is required, the studded bracket type is recommended.
- To maximize the uplift load resistance, high ρ_x percentages and low a/d ratios should be used for all bracket types, along with the middle or top h_e for the single bracket type.
- Overall uplift behavior of double and studded bracket types is comparable to middle or top h_e of single bracket type, and the load capacity obtained for these brackets are similar within a range of $\pm 5\%$.

Compression Behavior

- No anchorage failure is predicted for compression loads in any of the bracket types.
- The compressive load capacity increases by an average of 24% when ρ_x is increased from 0.2% to 0.4% or from 0.4% to 0.8% for the single bracket type.
- The compressive load capacity increases by an average of 25% when the a/d ratio is decreased from 1.68 to 1.42 or from 1.42 to 1.11 for the single bracket type.
- The double and studded bracket types exhibit load capacity increases similar to the single bracket type for similar changes in ρ_x or a/d ratios.
- To maximize the compressive load resistance, high ρ_x percentages and low a/d ratios is recommended, regardless of the h_e for all bracket types.

ACKNOWLEDGEMENT

The authors would like to thank Helical Piles and Tiebacks Committee of the Deep Foundation Institute (DFI) for providing funding for this study.

REFERENCES

- ACI Committee 318, 2014. Building code requirements for structural concrete (ACI 318-14) and commentary (ACI 318R-14), American Concrete Institute, Farmington Hills, MI, USA, 524 p.
- Adebar, P., Kuchma, D., and Collins, M.P., 1990. Strut-and-tie models for the design of pile caps: an experimental study. *American Concrete Institute Structural Journal*, 87(1): 81-92. Retrieved from <https://trid.trb.org/view/307069> Accessed 23/03/2019.
- Akkaya, Y., Guner, S., and Vecchio, F.J., 2019. A constitutive model for the inelastic buckling behavior of reinforcing bars. *ACI Structural Journal*, 116(3): 195-204. Retrieved from http://www.utoledo.edu/engineering/faculty/serhan-guner/docs/JP11_Akkaya_et_al_2019.pdf Accessed 23/03/2019.
- Cao, J., 2009. The shear behaviour of the reinforced concrete four-pile caps. Ph.D. Thesis, School of Civil Engineering and the Environment, University of Southampton, Southampton, UK, 287 p. Retrieved from <https://eprints.soton.ac.uk/73699/> Accessed 23/03/2019.
- Cerato, A., and Victor, R., 2009. Effects of long-term dynamic loading and fluctuating water table on helical anchor performance for small wind tower foundations. *Journal of Performance of Constructed Facilities*, 23(4): 251-26. [https://doi.org/10.1061/\(ASCE\)CF.1943-5509.0000013](https://doi.org/10.1061/(ASCE)CF.1943-5509.0000013)
- CRSI., 2015. Design guide for pile caps (1st ed.). Concrete Reinforcing Steel Institute, Schaumburg, IL, 156 p. Retrieved from <http://resources.crsi.org/resources/design-guide-for-pile-caps/> Accessed 23/03/2019.
- Diab, M.A.M., 2015. Behavior of helical pile connectors for new foundations. Ph.D. Thesis, School of Civil and Environment Engineering, University of Western Ontario, London, Ontario, Canada, 638 p. Retrieved from <https://ir.lib.uwo.ca/cgi/viewcontent.cgi?article=4736&context=etd> Accessed 23/03/2019.
- Elkasabgy, M., and El Naggar, M.H., 2013. Dynamic response of vertically loaded helical and driven steel piles. *Canadian Geotechnical Journal*, 50(5): 521–535. <https://doi.org/10.1139/cgj-2011-0126>
- El Naggar, M.H., Youssef, M.A., and Ahmed, M., 2007. Monotonic and cyclic lateral behaviour of helical pile specialized connectors. *Engineering Structures*, 29(10): 2635–2640. <https://doi.org/10.1016/j.engstruct.2007.01.018>
- Elsherbiny, Z.H., and El Naggar, M.H., 2013. Axial compressive capacity of helical piles from field tests and numerical study. *Canadian Geotechnical Journal*, 50(12): 1191–1203. <https://doi.org/10.1139/cgj-2012-0487>
- Guner, S., and Carrière, J., 2016. Analysis and strengthening of caisson foundations for uplift loads. *Canadian Journal of Civil Engineering*, 43(5): 411–419. Retrieved from <http://www.utoledo.edu/engineering/faculty/serhan-guner/docs> Accessed 23/03/2019.

Labuda, T., Corley, G.W., and Murphy, M., 2013. Failure investigation of a helical anchor tie-down system supporting an olympic size swimming pool. Proceedings of the Seventh International Conference on Case Histories in Geotechnical Engineering, Chicago, April 29-May 4, Scholoars' Mine, Missouri University of Science and Technology. 7 p. Retrieved from <http://scholarsmine.mst.edu/cgi/viewcontent.cgi?article=3223&context=icchge> Accessed 23/03/2019.

Livneh, B., and El Naggar, M.H., 2008. Axial testing and numerical modeling of square shaft helical piles under compressive and tensile loading. Canadian Geotechnical Journal, 45(8): 1142-1155. <https://doi.org/10.1139/T08-044>

Otsuki, K., and Suzuki, K., 1996. Experimental study on bending ultimate strength of four-pile caps. Trans Jpn Concrete Inst, 482: 93-102. Retrieved from <https://ci.nii.ac.jp/naid/110004303171> Accessed 23/03/2019.

Suzuki, K., Otsuki, K., and Tsubata, T., 2000. Influence of edge distance on failure mechanism of pile caps. Trans Jpn Concrete Inst, 22: 361-367. Retrieved from <https://ci.nii.ac.jp/naid/10007467724/> Accessed 23/03/2019.

Suzuki, K., and Otsuki, K., 2002. Experimental study on corner shear failure of pile caps. Trans Jpn Concrete Inst, 23: 303-310. Retrieved from <https://ci.nii.ac.jp/naid/10007251043/> Accessed 23/03/2019.

Vecchio, F.J., and Collins, M.P., 1986. The modified compression field theory for reinforced concrete elements subject to shear. ACI Journal, 83(2): 219–231. <https://doi.org/10.14359/10416>

Vecchio, F.J., 2000. Disturbed stress field model for reinforced concrete: formulation. Journal of Structural Engineering, 126(8): 1070–1077. [https://doi.org/10.1061/\(asce\)0733-9445\(2000\)126:9\(1070\)](https://doi.org/10.1061/(asce)0733-9445(2000)126:9(1070))

VTAG, 2019. VecTor2: Nonlinear finite element analysis software for reinforced concrete structures. VecTor Analysis Group (VTAG) Version 2.9 (Online), Retrieved from <http://vectoranalysisgroup.com/> Accessed 23/03/2019.

Wong P.S., Vecchio F.J., and Trommels H., 2013. VecTor2 and formworks user's manual. Technical Report, Department of Civil Engineering, University of Toronto, ON, Canada, 347 p. Retrieved from http://www.vectoranalysisgroup.com/user_manuals/manual1.pdf Accessed 23/03/2019.

Youssef, M.A., El Naggar, M.H., and Ahmed, M., 2006. Monotonic and cyclic load behaviour of helical pile connectors in the vertical direction. Canadian Journal of Civil Engineering, 18(1996): 10–18. <https://doi.org/10.1139/l05-074>